Supporting Information

Aromatic fluorocopolymers based on α-(difluoromethyl)styrene and styrene: Synthesis and characterization, and thermal and surface properties

Joanna Wolska,[1] Justyna Walkowiak-Kulikowska,[1,] Anna Szwajca,[1]*

Henryk Koroniak,[1] Bruno Améduri,[2,]*

[1] Adam Mickiewicz University, Faculty of Chemistry, Umultowska 89b, 61-614 Poznań, Poland

[2] Institut Charles Gerhardt, Ingénierie et Architectures Macromoléculaires, UMR CNRS 5253, ENSCM, University of Montpellier, Palace Eugene Bataillon, 34095 Montpellier, France

Table of content

1. Synthesis of *α*-(difluoromethyl)styrene (DFMST)

The most convenient grams scale synthesis of *α*-(difluoromethyl)styrene (DFMST) began with acetophenone **1** (Scheme 1 in main manuscript). Base-induced difluoromethylation coupling was performed reacting ketone **1** with difluoromethylphenyl sulfone **2** ($PhSO_2CF_2H$) in the presence of excess of lithium bis(trimethylsilyl)amide (LiHMDS) and led to the formation of desired 1,1-difluoro-2-phenyl-1-(phenyl-sulfonyl)propan-2-ol **3**. However, a duration of base addition had a crucial impact on the efficiency of this step. The resulting product was isolated with excellent (94%) yield (lit. 74%) [1]. Alcohol **3** was converted using reductive desulfonylation into 1,1-difluoro-2-phenylopropan-2-ol **4** in 86% yield (lit. 93%) [2]. The mechanism of the reduction proposed by Prakash *et al*. [2] involved a transfer of an electron from a magnesium atom to sulfur atom of phenylsulfonic group. Metallic magnesium used as a reducing agent, was activated by AcOH–NaOAc buffer. Concentration of the buffer and composition of solvents used in the reaction influenced considerably the process yield. Dehydration of resulting carbinol **4** using phosphorus pentoxide afforded the desired *α*-(difluoromethyl)styrene **5** in 69% yield [3].

This three-step synthetic route towards *α*-(difluoromethyl)styrene using a nucleophilic difluoromethylation followed by reductive desulfonylation and subsequent dehydration was found to be selective, cost-effective, easy to implement and easily scalable (up to 22 mmol) giving the desired *gem*-difluorinated styrenic monomer in 56% overall yield.

1.1. Synthetic procedure of *α*-(difluoromethyl)styrene (DFMST) [3]

1.1.1. 1,1-Difluoro-2-phenyl-1-(phenylsulfonyl)propan-2-ol (3)

To a solution of difluoromethyl phenyl sulfone, $PhSO_2CF_2H$ (4.24 g, 22.1 mmol) and acetophenone (5.31 g, 5.15 mL, 44.1 mmol) in THF/HMPA (v/v, 10:1) cooled to -78 °C was added dropwise LiHMDS (1M in THF, 44.1 mL, 44.1 mmol). Reaction was stirred at -78 °C for 6 h. Saturated aqueous NaCl (440 mL) was then added at -78 °C, then the residue was brought to room temperature and extracted with Et_2O (3 × 440 mL). The combined organic layers were dried over Na_2SO_4 and concentrated under reduced pressure. The crude product was purified by silica gel column chromatography using hexane and ethyl acetate as eluents (6:1). R_f = 0.30 (hexane:ethyl acetate, 6:1), giving 6.52 g (20.8 mmol, 94%) of 1,1-difluoro-2-phenyl-1-(phenylsulfonyl)-propan-2-ol as colorless thick oil/white solid (m.p. 76-80°C). **^{1}H NMR** (400 MHz, $CDCl_3$): δ (ppm) 7.87 (d, $^3J_{H\text{-}H}$ = 7.8 Hz, 2H, H_{Ar}), 7.74-7.66 (m, 1H, H_{Ar}), 7.61-7.48 (m, 4H, H_{Ar}), 7.41-7.29 (m, 3H, H_{Ar}), 3.85 (s, 1H, O*H*), 1.96 (t, $^4J_{H\text{-}H}$ = 1.3 Hz, 3H, CH_3); **^{13}C NMR** (100 MHz, $CDCl_3$): δ (ppm): 138.3 (s, C_{Ar}), 135.8 (s, C_{Ar}), 134.2 (s, C_{Ar}), 130.8 (s, C_{Ar}), 129.6 (s, C_{Ar}), 129.0 (s, C_{Ar}), 128.6 (s, C_{Ar}), 127.0 (s, C_{Ar}), 121.4 (t, $^1J_{C\text{-}F}$ = 298.4 Hz, CF_2), 77.3 (t, $^2J_{C\text{-}F}$ = 21.2 Hz, (OH)CCF_2), 25.36 (s, CH_3); **^{19}F NMR** (376 MHz, $CDCl_3$): δ (ppm) -105.9 (s, 2F, CF_2).

1.1.2. 1,1-Difluoro-2-phenylpropan-2-ol (4)

To a mixture of AcOH/NaOAc (1:1) buffer solution (119 mL, 8 mol/L) and DMF (322 mL) at room temperature was added 1,1-difluoro-2-phenyl-1-(phenylsulfonyl)propan-2-ol (6.51 g, 20.9 mmol). Magnesium turnings (12.7 g, 521.0 mmol) were added in portionwise. The reaction mixture was stirred at room temperature for 4 h followed by addition of water (625 mL). The solution mixture was extracted with Et_2O (3 × 450 mL), and the combined organic phase was washed with saturated $NaHCO_3$ solution and brine, and then dried over Na_2SO_4. After the removal of Et_2O, the crude product was purified by silica gel column chromatography using hexane and ethyl acetate as eluents (5:1). R_f = 0.43 (hexane:ethyl acetate, 5:1), giving 3.10 g (18.0 mmol, 86%) of 1,1-difluoro-2-phenylpropan-2-ol as colorless liquid. **^{1}H NMR** (400 MHz, $CDCl_3$): δ (ppm): 7.57-7.45 (m, 2H, H_{Ar}), 7.44-7.27 (m, 3H, H_{Ar}), 5.71 (dd, $^2J_{H\text{-}F}$ = 56.7, 56.2 Hz, 1H, CF_2H), 2.37 (s, 1H, O*H*), 1.65 (t, $^4J_{H\text{-}H}$ = 1.6 Hz, 3H, CH_3); **^{13}C NMR** (100 MHz, $CDCl_3$): δ (ppm): 140.5 (s, C_{Ar}), 128.5 (s, C_{Ar}), 128.2 (s, C_{Ar}), 125.9 (s, C_{Ar}), 117.0 (t, $^1J_{C\text{-}F}$ = 249.1 Hz, CF_2H), 74.3 (t, $^2J_{C\text{-}F}$ = 22.0 Hz, (OH)CCF_2), 22.3 (s, CH_3); **^{19}F NMR** (376 MHz, $CDCl_3$): δ (ppm) -129.8 (dd, $^2J_{F\text{-}F}$ = 276.1 Hz, $^2J_{H\text{-}F}$ = 56.2 Hz, 1F, CF_2H), -131.1 (dd, $^2J_{F\text{-}F}$ = 276.1 Hz, $^2J_{H\text{-}F}$ = 56.8 Hz, 1F, CF_2H).

1.1.3. *α*-(Difluoromethyl)styrene (DFMST) (5)

To a solution of 1,1-difluoro-2-phenylpropan-2-ol (3.10 g, 18.0 mmol) in toluene (36 mL) was added P_2O_5 (1.28 g, 9.02 mmol) and the mixture was stirred at reflux for 5 h. The reaction was then allowed to cool to room temperature and poured into a separating funnel charged with water (250 mL). After extracting with pentane (3 × 300 mL), the combined organic layers were dried over Na_2SO_4 and concentrated under reduced pressure. The residue was purified by short-path distillation under reduced pressure (b.p. 53-55 °C, 9-11 mbar), giving 1.90 g (12.32 mmol, 81%) of DFMST as colorless liquid. **^{1}H NMR** (400 MHz, $CDCl_3$): δ (ppm): 7.51 (d, $^3J_{H\text{-}H}$ = 6.3 Hz, 2H, H_{Ar}), 7.46-7.35 (m, 3H,

H_{Ar}), 6.42 (t, $^{2}J_{H\text{-}F}$ = 55.3 Hz, 1H, CF_2H), 5.75 (s, 1H, C=CH_2), 5.69 (s, 1H, C=CH_2); **^{13}C NMR** (100 MHz, $CDCl_3$): δ (ppm): 141.9 (t, $^{2}J_{C\text{-}F}$ = 19.9 Hz, H_2C=$C$$CF_2H$), 134.7 (s, C_{Ar}), 128.6 (s, C_{Ar}), 128.5 (s, C_{Ar}), 126.9 (s, C_{Ar}), 118.9 (t, $^{3}J_{C\text{-}F}$ = 9.5 Hz, H_2C=CCF_2H), 115.4 (t, $^{1}J_{C\text{-}F}$ = 239.6 Hz, CF_2H); **^{19}F NMR** (376 MHz, $CDCl_3$): δ (ppm) -113.6 (d, $^{2}J_{H\text{-}F}$ = 55.3 Hz, 2F, CF_2H).

2. Homopolymerization of DFMST

The homopolymerizations were carried out in bulk using freshly distilled DFMST. Summary data was presented in Table S1. No viscosity increase was noted in these homopolymerizations. The ^{1}H NMR spectroscopy confirmed that all approaches to obtain poly(DFMST) homopolymer failed, and did not even lead to any oligomers.

Table S1: Attempted free radical homopolymerizations of DFMST

Entry	Initiator[a]	Monomer in feed [mol]	Initial mol % of initiator	Temperature [°C]	Time [h]	Monomer conversion [%][b]
1	AIBN	0.0065	1	60	20	0
2	AIBN	0.0065	2	60	20	0
3	AIBN	0.0065	1	70	20	0
4	AIBN	0.0130	1	70	20	0
5	BPO	0.0065	1	70	20	0
6	BPO	0.0065	2	70	20	0
7	BPO	0.0065	1	90	20	0
8	BPO	0.0130	1	90	20	0

[a] *α*,*α*′-Azobis(isobutyronitrile) (AIBN), benzoyl peroxide (BPO).

[b] Determined by ^{1}H NMR spectroscopy.

3. Spectroscopic characterizations of poly(*α*-(difluoromethyl)styrene-*co*-styrene) copolymers

3.1. Description of ST and DFMST monomers ^{1}H NMR spectra presented in Figure 1 (main manuscript)

The ^{1}H NMR spectrum of ST (—) exhibited signals at 5.46 ppm (dd, $^{3}J_{H\text{-}H}$ = 10.9 Hz, $^{2}J_{H\text{-}H}$ = 28 Hz), 5.97 ppm (dd, $^{3}J_{H\text{-}H}$ = 17.6 Hz, $^{2}J_{H\text{-}H}$ = 28 Hz) and 6.94 ppm (dd, $^{3}J_{H\text{-}H}$ = 17.6 Hz, $^{3}J_{H\text{-}H}$ = 10.9 Hz) assigned to vinyl protons H_2, H_3 and H_1, respectively and characteristic multiplets attributed to aromatic protons of monosubstituted benzene ring could have been at 7.45, 7.52 and 7.62 ppm. In that of DFMST (—), the characteristic triplet at 6.39 ppm attributed to -CF_2H group was observed (H_1), beside similar chemical shifts for vinyl protons H_2 and H_3 (centered at 5.75 and 5.69 ppm), as well as for aromatic protons at 7.51 and 7.40 ppm.

3.2. ^{1}H NMR spectra of poly(DFMST-*co*-ST) copolymers

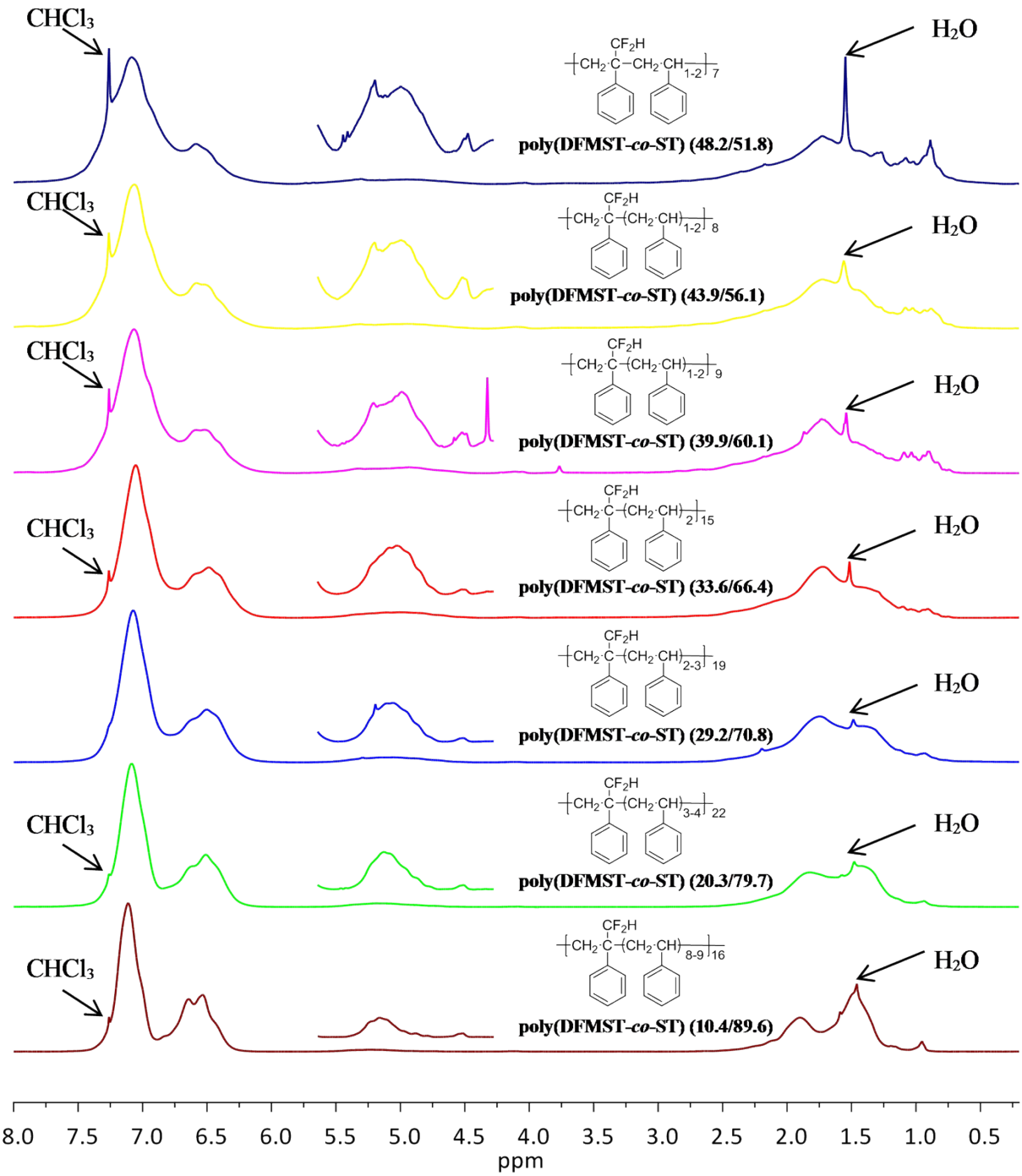

Fig. S1. Stack of ^{1}H NMR spectra (recorded in $CDCl_3$) of poly(DFMST-*co*-ST) copolymers with decreasing of DFMST comonomer units in polymer structure.

The ^{1}H NMR spectra of the poly(DFMST-*co*-ST) copolymers exhibit characteristic broad signals centered at 5.05 ppm attributed to the side chain primary proton of the difluoromethyl

group of DFMST units. Although fluorine atoms of such $–CF_2H$ group are not electronically equal due to the vicinity of the stereogenic carbon center, in the ^1H NMR spectra of copolymers signal of its proton will never be seen as triplet (t) or doublet of doublets (dd) since there is only one proton in comparison to all others from aromatic and aliphatic parts of polymer of both DFMST and ST units. In addition, usually a small amount of DFMST units was incorporated into the polymer chain. Moreover, the resonance line should be split into at least 3 (t) or even 4 (dd) lines what makes the multiplicity of the signal very difficult to recognize.

3.3. ^{19}F NMR spectra of poly(DFMST-*co*-ST) copolymers

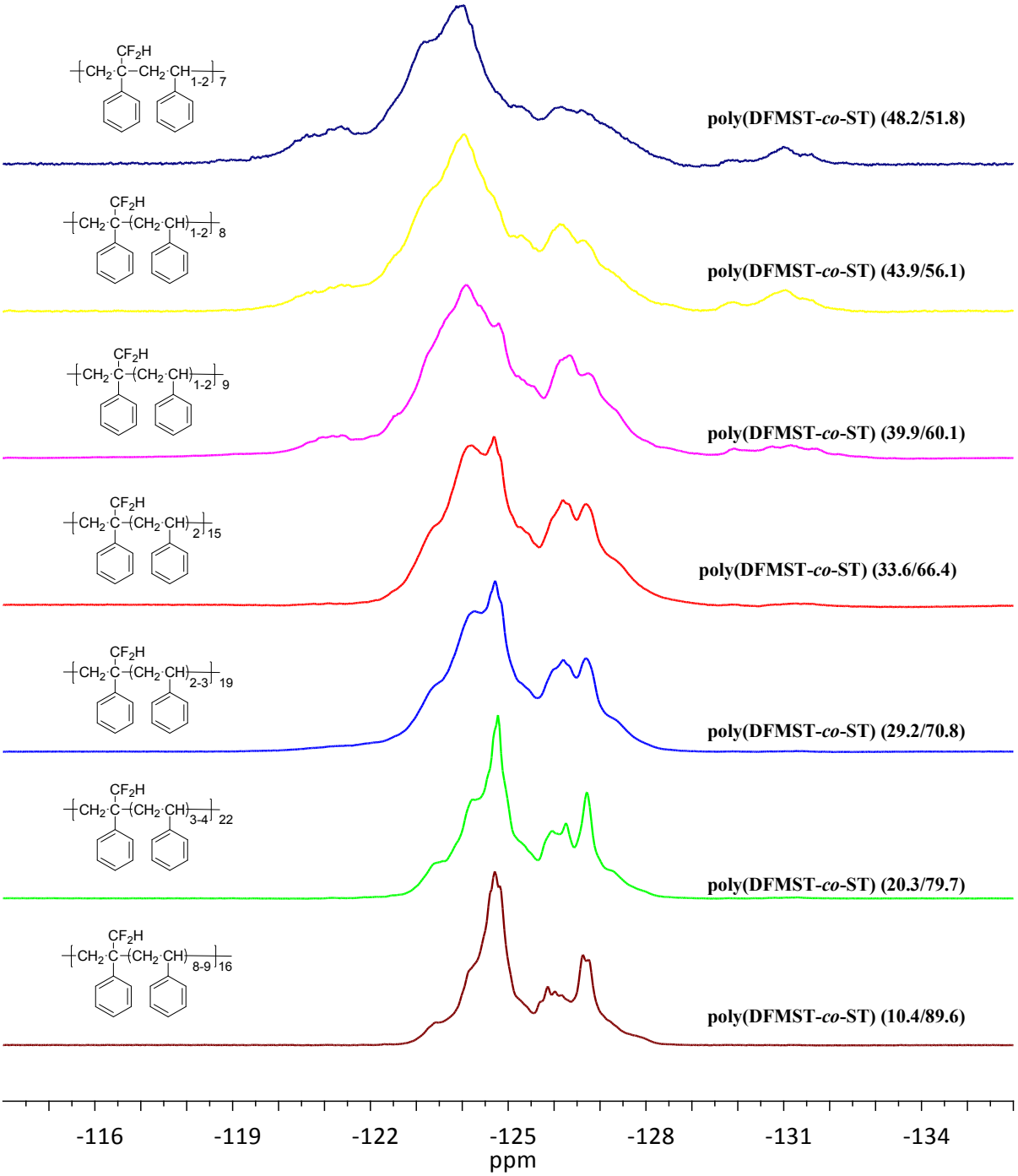

Fig. S2. Stack of ^{19}F NMR spectra (recorded in $CDCl_3$) of poly(DFMST-*co*-ST) copolymers with decreasing of DFMST comonomer units in polymer structure.

The stack of ^{19}F NMR spectra of poly(DFMST-*co*-ST) copolymers shows the $\{^1H\}$ decoupled spectra. The signals of AB system are observed since both fluorine atoms are not electronically equal due to the vicinity of the stereogenic carbon center. Therefore, two signals in the ^{19}F NMR spectrum of copolymer can be recognized. However, these are not two electronically different fluorine atoms from one difluoromethyl group. The significant difference in signals integration indicates that in our case these are two signals of two $-CF_2H$ groups with different vicinity/neighborhood. Each of the signals can be consider as two doublets of AB system (CF_xF_yH) with the gradual reduction of intensities of the outer lines in favors of the inner lines, a characteristic "sloping" or "tenting" towards the coupling partner.

3.4. ^{13}C NMR spectra of poly(DFMST-*co*-ST) copolymers

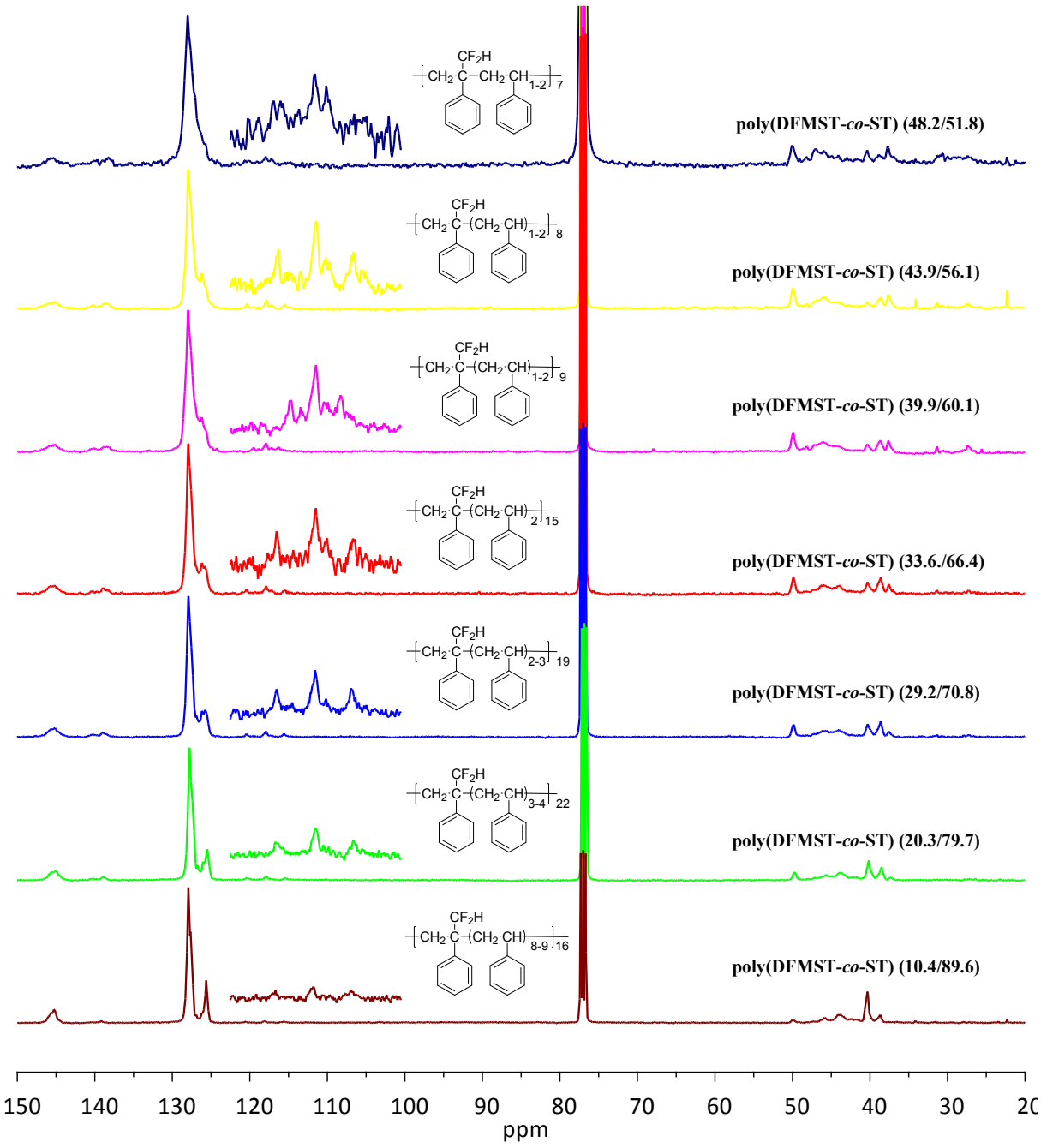

Fig. S3. Stack of ^{13}C NMR spectra (recorded in $CDCl_3$) of poly(DFMST-*co*-ST) copolymers with decreasing of DFMST comonomer units in polymer structure.

3.4.1. Description of poly(DFMST-*co*-ST) ^{13}C NMR spectra (Figure S3)

All the ^{13}C NMR spectra of poly(DFMST-*co*-ST) copolymers show characteristic broad triplet ($^{1}J_{C\text{-}F}$ = 246 Hz) centered at 117 ppm assigned to aliphatic difluoromethyl group (-CF_2H) ($C_{A'}$). These spectra also display expected multiplets centered at 39.3, 45.0 and 50.0 ppm corresponding to secondary, tertiary, and quaternary aliphatic carbons (C_A, C_B and $C_{B'}$) as well as multiplets centered at 126.5 and 142.7 ppm attributed to aromatic carbons of DFMST and ST units (C_C, C_D, C_E, $C_{C'}$, $C_{D'}$ and $C_{E'}$).

4. Determination of comonomer contents in poly(DFMST-*co*-ST) obtained in bulk radical copolymerization of DFMST with ST

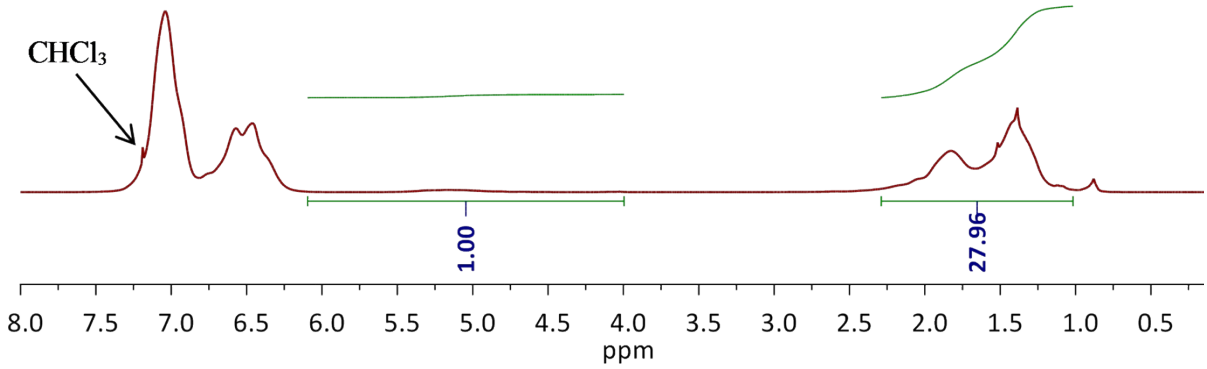

Fig. S4. ^{1}H NMR spectrum (recorded in $CDCl_3$) of poly(DFMST-*co*-ST) copolymer (10.4/89.6, M_n = 17 200 g mol^{-1})

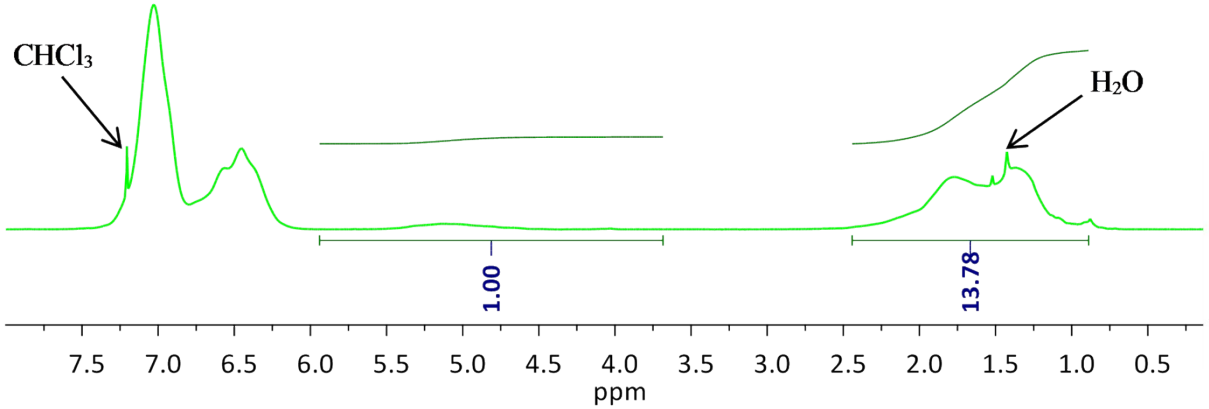

Fig. S5. ^{1}H NMR spectrum (recorded in $CDCl_3$) of poly(DFMST-*co*-ST) copolymer (20.3/79.7, M_n = 12 300 g mol^{-1})

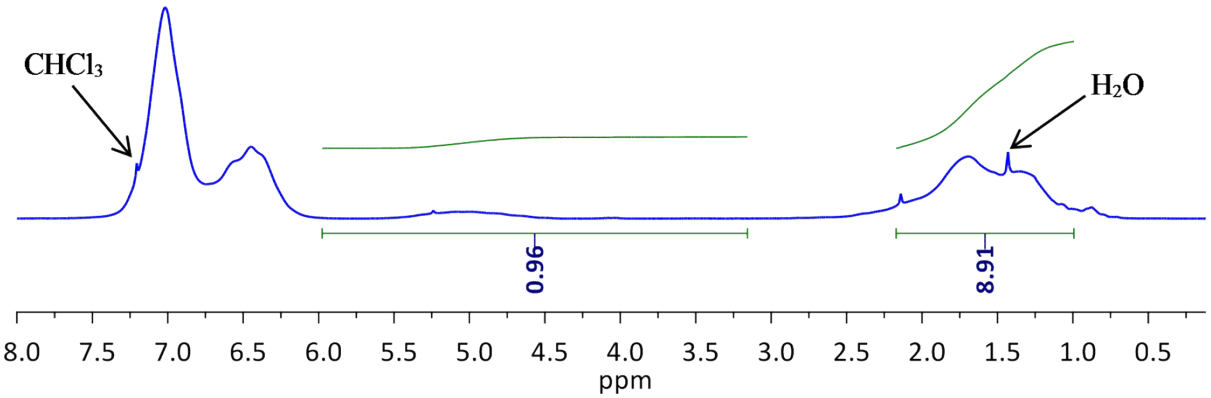

Fig. S6. ^{1}H NMR spectrum (recorded in $CDCl_3$) of poly(DFMST-*co*-ST) copolymer (29.2/70.8, M_n = 7 800 g mol^{-1})

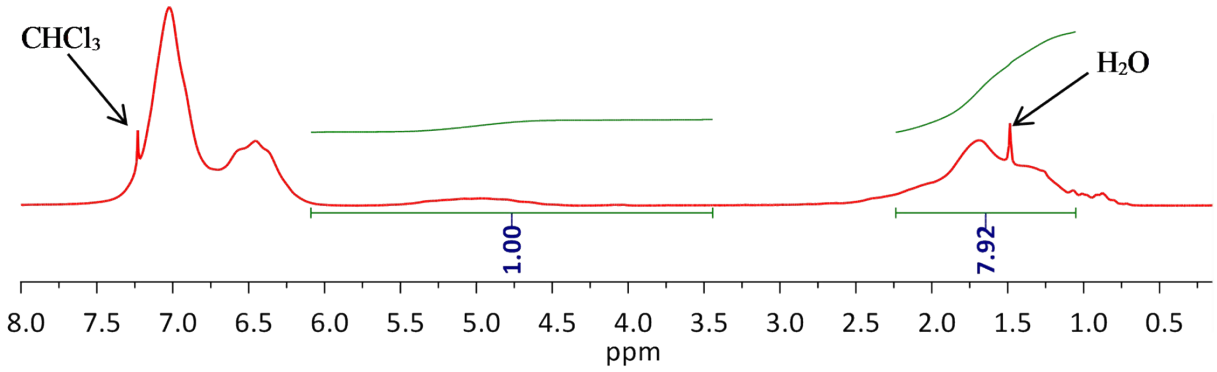

Fig. S7. ^{1}H NMR spectrum (recorded in $CDCl_3$) of poly(DFMST-*co*-ST) copolymer (33.6/66.4, M_n = 5 400 g mol^{-1})

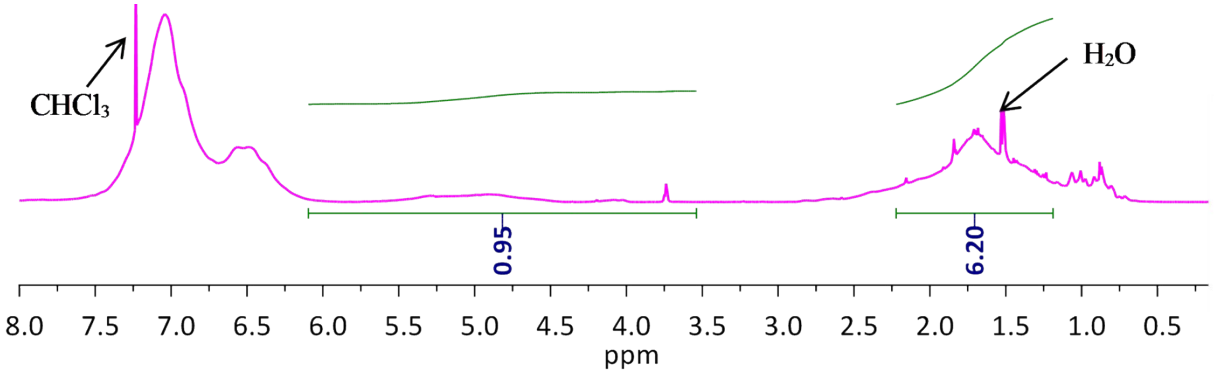

Fig. S8. ^{1}H NMR spectrum (recorded in $CDCl_3$) of poly(DFMST-*co*-ST) copolymer (39.9/60.1, M_n = 2 700 g mol^{-1})

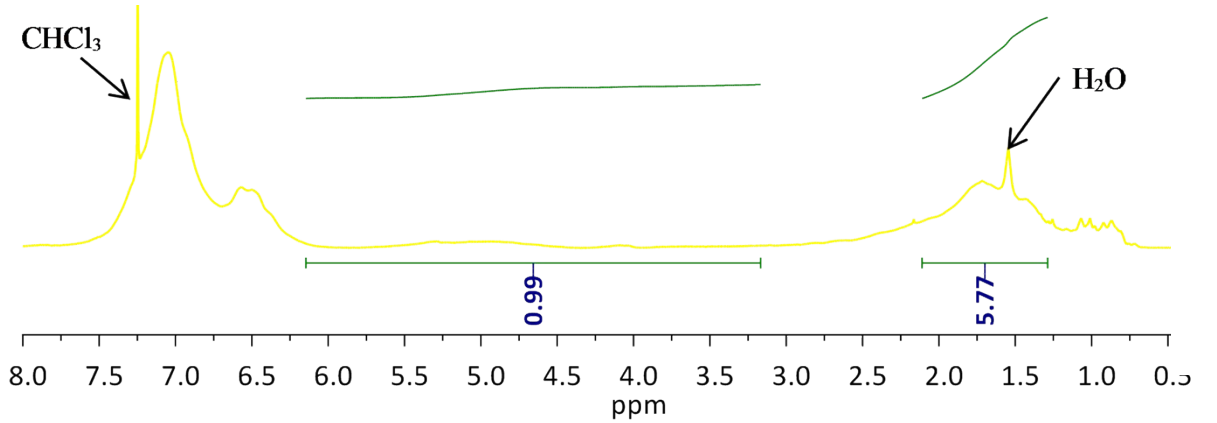

Fig. S9. ^{1}H NMR spectrum (recorded in $CDCl_3$) of poly(DFMST-*co*-ST) copolymer (43.9/56.1, M_n = 2 300 g mol^{-1})

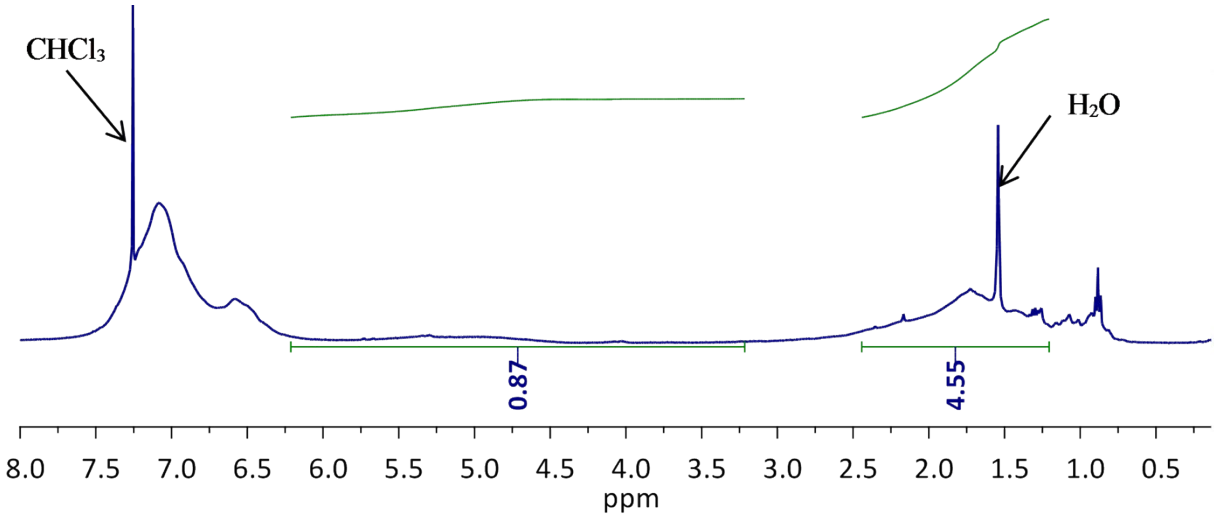

Fig. S10. ^{1}H NMR spectrum (recorded in $CDCl_3$) of poly(DFMST-*co*-ST) copolymer (48.2/51.8, M_n = 1 900 g mol^{-1})

Table S2: Determination of copolymer composition and number of units in poly(DFMST-*co*-ST) copolymers

Entry	$I_{A,B,B'}$	$I_{A'}$	$\%_{DFMST}/\%_{ST}$	$\%_{DFMST}$	$\%_{ST}$	M_n [g mol^{-1}]	$\#_{DFMST}$	$\#_{ST}$	No. (-$CH_2CH(Ph)$-) moieties
1	27.96	1.00	0.1156	10.0	90.0	17200	16	141	157
2	13.78	1.00	0.2547	20.0	80.0	12300	22	86	108
3	8.91	0.96	0.4120	29.2	70.8	7800	19	47	66
4	7.92	1.00	0.5068	33.6	66.4	5400	15	30	45
5	6.20	0.95	0.6628	39.9	60.1	2700	9	13	22
6	5.77	0.99	0.7836	43.9	56.1	2300	8	10	18
7	4.55	0.87	0.9288	48.2	51.8	1900	7	8	15

$$mol\%_{ST} = [(I_{A,B,B'} - I_{A'}) / 3] / ([(I_{A,B,B'} - I_{A'}) / 3] + I_{A'})$$

$$mol\%_{DFMST} = (I_{A'}) / ([(I_{A,B,B'} - I_{A'}) / 3] + I_{A'})$$

where $I_{A,B,B'}$ and $I_{A'}$ stand for the integrals of the signals centered at 1.59 ppm and 5.00 ppm, respectively.

Number of ST units in copolymer $\#_{ST} = M_n / (M_{ST} + [(\%_{DFMST} / \%_{ST}) \cdot M_{DFMST}])$

number of DFMST units in copolymer $\#_{DFMST} = \#_{ST} \cdot (\%_{DFMST} / \%_{ST})$

where M_{ST} and M_{DFMST} stand for molecular weights of ST (104.15 g mol^{-1}) and DFMST (154.16 g mol^{-1}), respectively.

5. Determination of reactivity ratios of DFMST and ST

The **Fineman-Ross law** (FR) uses the following equation:

$$G = r_1 H - r_2$$

With $G = x(X-1)$ and $H = x^2/X$.

Where, $x = f_1/f_2$ stands for the feed monomers composition,

$X = F_1/F_2$ stands for the copolymer composition.

The obtained G and H from above equations will result in the plot (G *versus* H), where the intercept gives $-r_2$ and its slope shows r_1.

When $r_1 = 0$, the equation simplifies to:

$$G = r_2 H$$

With $G = (1-X)$ and $H = X/x$.

The obtained G and H from above equations will result in the plot (G *versus* H), where the $r_1 = 0$ and the slope shows r_2.

The **Inverted Fineman-Ross method** (IFR) is based on the following equation:

$$G/H = r_1 - (1/H) r_2$$

And G and H defined by Fineman-Ross method (see above).

The obtained G and H from above equations will result in the plot (G/H *versus* 1/H), where the intercept gives r_1 ($r_1 = 0$, since plot crosses the zero point) and its slope shows $-r_2$.

The **Kelen-Tüdős law** (KT) uses the following equation:

$$\eta = (r_1 + r_2/\alpha)\xi - r_2/\alpha$$

With $\eta = G/(\alpha + H)$ and $\xi = H/(\alpha + H)$ and $\alpha = (H_{min} \times H_{max})^{1/2}$

And G and H defined by Fineman-Ross method (see above)

The obtained η and ξ from above equations will result in the plot (η *versus* ξ), where r_2 is calculated from the negative value of intercept multiplied by α (r_2 = -"intercept" × α) and the slope minus intercept gives r_1.

When $r_1 = 0$, the equation simplifies to:

$$\eta = r_2/\alpha(\xi\text{-}1)$$

With $\eta = G/(\alpha + H)$ and $\xi = H/(\alpha + H)$ and $\alpha = (H_{min} \times H_{max})^{1/2}$

The obtained η and ξ from above equations will result in the plot (η *versus* ξ), where the intercept gives r_1 ($r_1 = 0$, since plot crosses the zero point) and r_2 is calculated from the slope multiplied by α (r_2 = "value of slope" × α).

The **Extended Kelen-Tüdős law** (EKT) uses the following equation:

$$\eta = (r_1 + r_2/\alpha)\xi - r_2/\alpha$$

With $\eta = z(X\text{-}1)/(\alpha z^2 + X)$ and $\xi = X/(\alpha z^2 + X)$ and $\alpha = (H_{min} \times H_{max})^{1/2}$

And $G = (X\text{-}1)/z$ and $H = X/z^2$

Where, $z = \log(1\text{-}\zeta_1)/\log(1\text{-}\zeta_2)$ stands for conversion-dependent value,

With $\zeta_2 = \zeta(1+x)/(1+X)$ and $\zeta_1 = (X/x)\zeta_2$

Where ζ_1 and ζ_2 are partial conversions of individual monomers, and while ζ stands for the experimental conversion given on the molar basis.

The obtained η and ξ from above equations will result in the plot (η *versus* ξ), where r_2 is calculated from the negative value of intercept multiplied by α (r_2 = -"intercept" × α) and the slope minus intercept gives r_1.

When $r_1 = 0$, the equation simplifies to:

$$\eta = r_2/\alpha(\xi\text{-}1)$$

With η, ξ, α, G, H, z, ζ_1, ζ_2 defined as described above for the extended Kelen-Tüdős method.

The obtained η and ξ from above equations will result in the plot (η *versus* ξ), where the intercept gives r_1 ($r_1 = 0$, since plot crosses the zero point) and r_2 is calculated from the slope multiplied by α ($r_2 =$ "value of slope" $\times \alpha$).

The **Mayo-Lewis method** (ML) uses the following equation:

$$r_2 = Hr_1 - G$$

And G and H defined by Fineman-Ross method (see above).

The cross-point of the lines plotted by considering arbitrary values for r_2 ($0.10 < r_1 < 1.00$) will result in the real amounts of reactivity ratios.

The **Yezrielev-Brokhina-Roskin law** (YBR) uses the following equation:

$$G = H^{3/2}r_1 - r_2$$

And G and H defined by Fineman-Ross method (see above).

The obtained G and $H^{3/2}$ from above equations will result in the plot (G *versus* $H^{3/2}$), where the slope shows r_1 and its intercept gives $-r_2$.

Table S3: Determination of (DFMST;ST) reactivity ratios, at 70 °C, by Mayo-Lewis (ML), Finemann-Ross (FR), Inverted Fineman-Ross (IFR), Kelen-Tüdős (KT), Extended Kelen-Tüdős (EKT), Yezrielev-Brokhina-Roskin (YBR) linear least-squares methods when r_{DFMST}=0.

Method	r_{DFMST}	r_{ST}
Mayo-Lewis	0.00	0.72 ± 0.30
Fineman-Ross	0.00	0.71 ± 0.07
Inverted Fineman-Ross	0.00	0.74 ± 0.14
Yezrielev-Brokhina-Roskin	0.00	0.64 ± 0.30
Kelen-Tüdős	0.00	0.74 ± 0.05
Extended Kelen-Tüdős (low conversion)	0.00	0.74 ± 0.02
Extended Kelen-Tüdős (high conversion)	0.00	0.69 ± 0.04

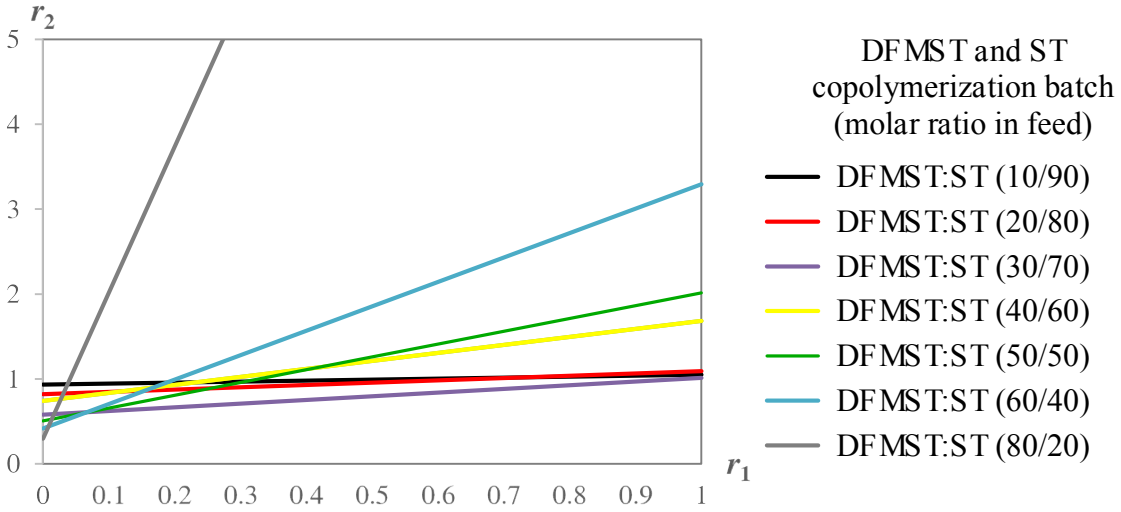

Figure S11. Mayo-Lewis linear least-squares method for the determination of the reactivity ratios of DFMST and ST.

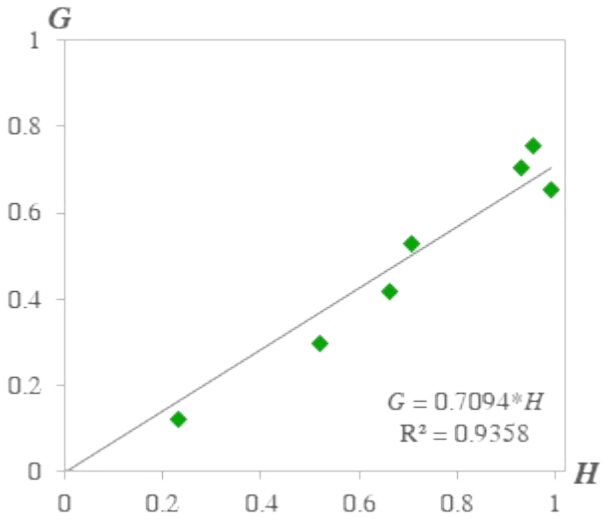

Figure S12. Fineman-Ross linear least-squares method for the determination of the reactivity ratios of DFMST and ST.

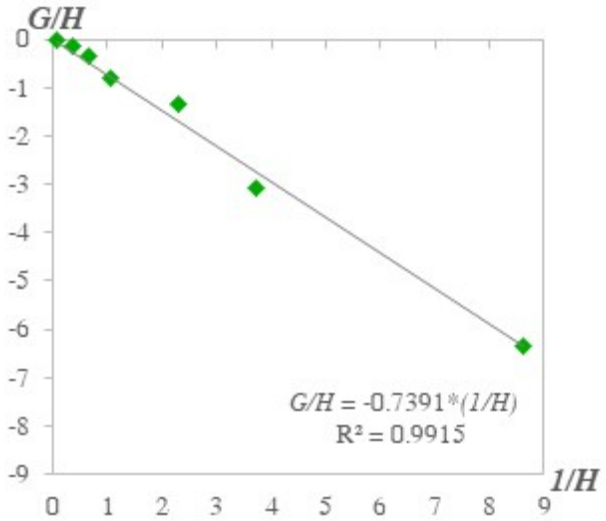

Figure S13. Inverted Fineman-Ross linear least-squares method for the determination of the reactivity ratios of DFMST and ST.

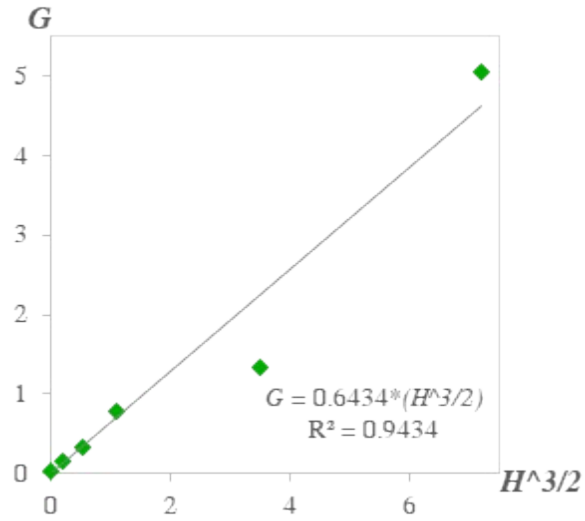

Figure S14. Yezrielev-Brokhina-Roskin linear least-squares method for the determination of the reactivity ratios of DFMST and ST.

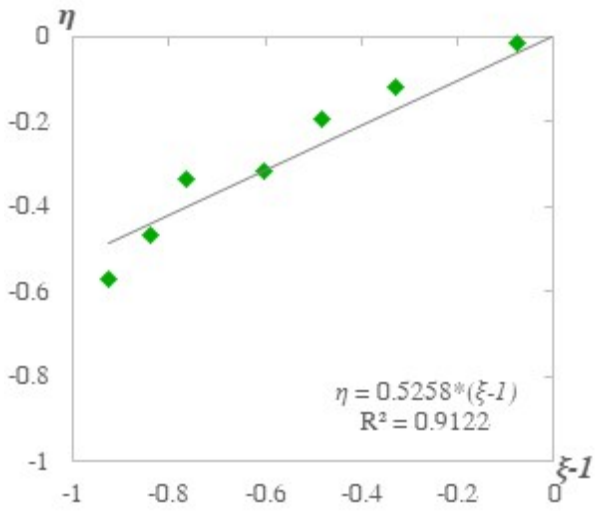

Figure S15. Kelen-Tüdős linear least-squares method for the determination of the reactivity ratios of DFMST and ST.

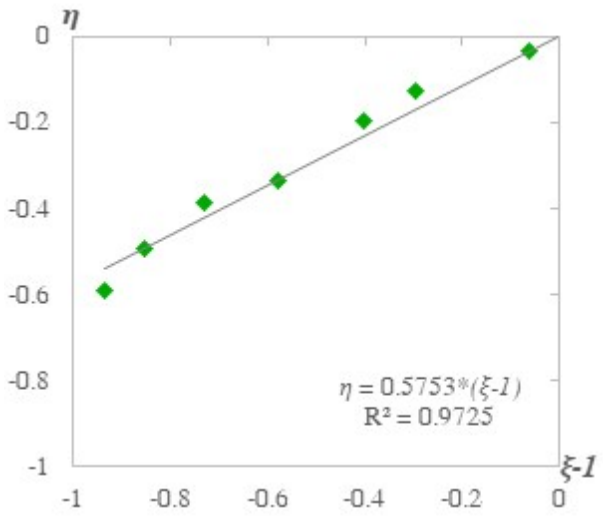

Figure S16. Extended Kelen-Tüdős linear least-squares method for the determination of the reactivity ratios of DFMST and ST at low conversions.

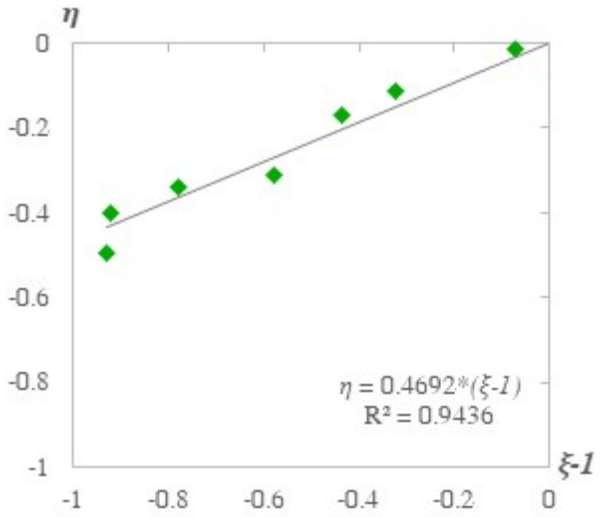

Figure S17. Extended Kelen-Tüdős linear least-squares method for the determination of the reactivity ratios of DFMST and ST at high conversions.

6. Determination of average molar masses of poly(DFMST-*co*-ST) copolymers from GPC with polystyrene standards

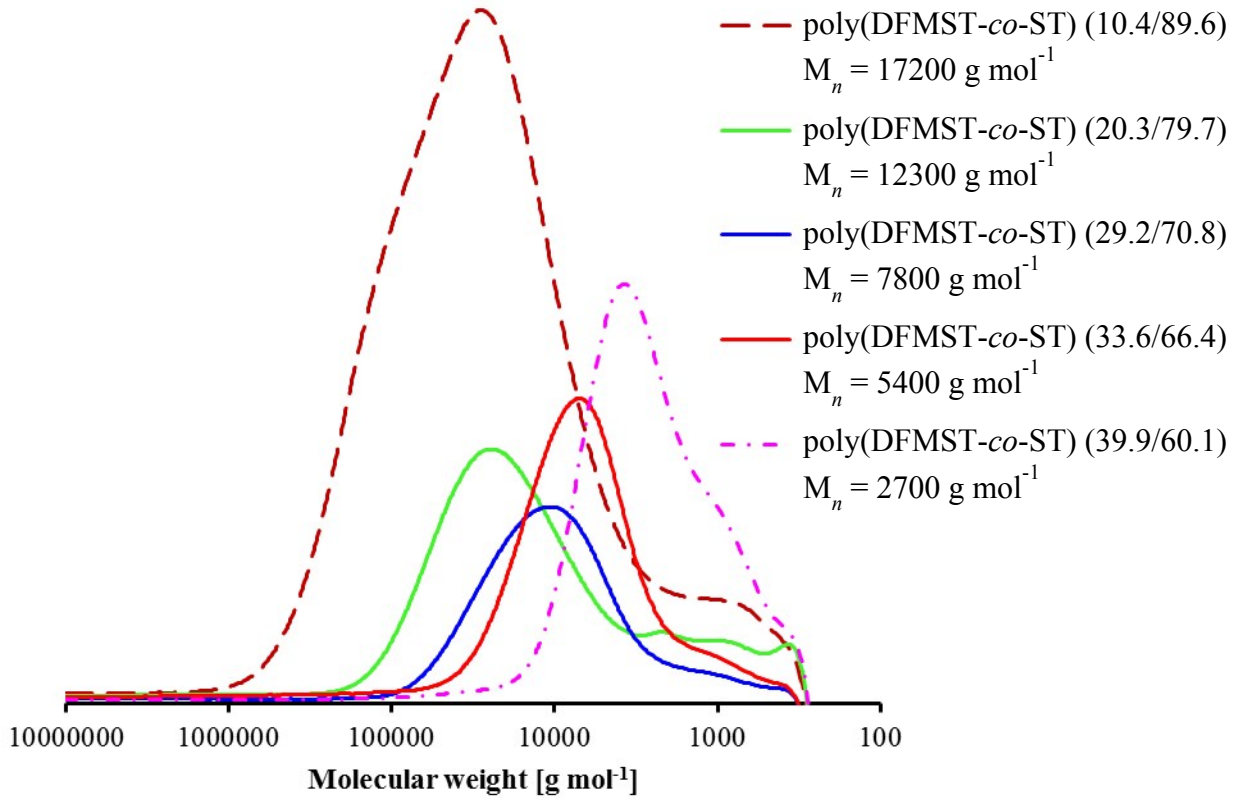

Fig. S18. GPC chromatograms of series poly(DFMST-*co*-ST) copolymers with different comonomer contents obtained in bulk radical copolymerizations.

Table S4: poly(DFMST-*co*-ST) copolymers average molecular weights (M_n, M_w) and dispersities (Đ) assessed from GPC with polystyrene standards.

Molar ratio in polymer [mol%]		M_n [g mol^{-1}]	M_w [g mol^{-1}]	Đ
DFMST	ST			
10.4	89.6	17300	53000	3.07
20.3	79.7	12300	25500	2.07
29.2	70.8	7800	14500	1.86
33.6	66.4	5400	8600	1.59
39.9	60.1	2700	4000	1.51
43.9	56.1	2300	4600	2.02
48.2	51.8	1900	2400	1.24

7. Thermal properties of poly(DFMST-*co*-ST) copolymers

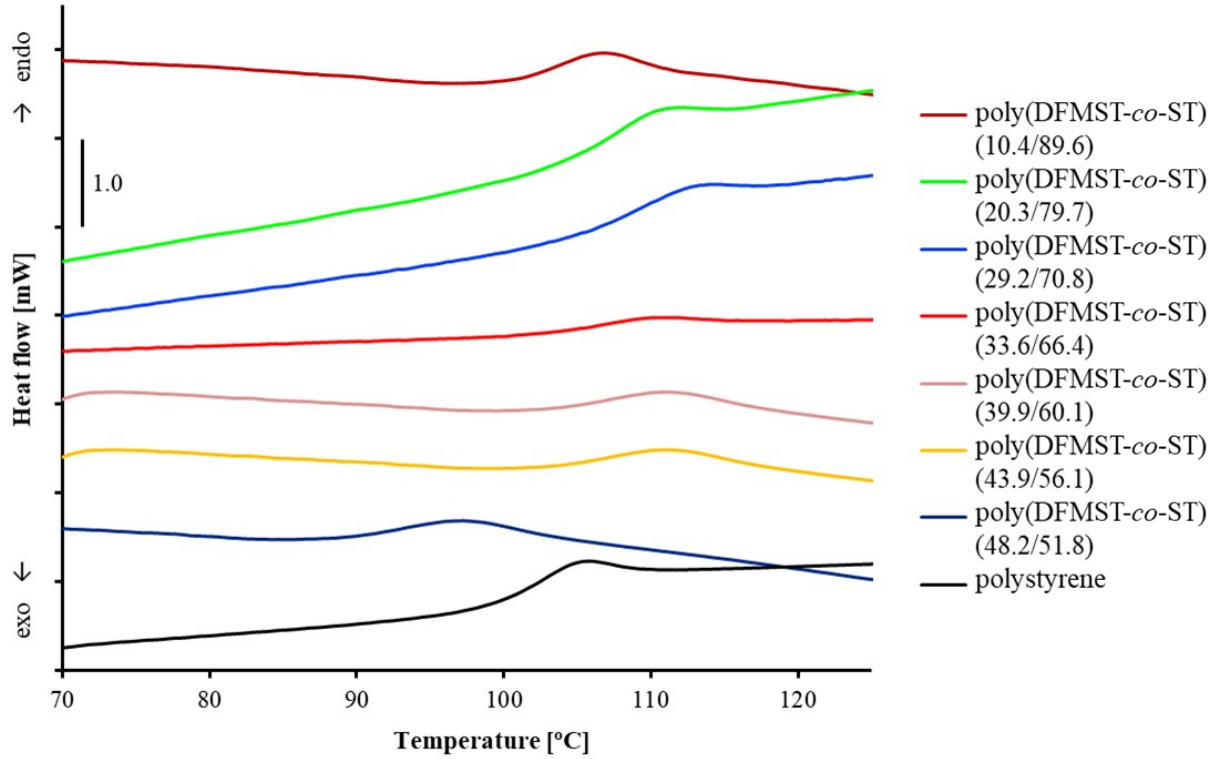

Fig. S19. DSC thermograms to highlight the glass transition temperatures (T_gs) of series poly(DFMST-*co*-ST) copolymers with different comonomer contents obtained in bulk radical copolymerizations.

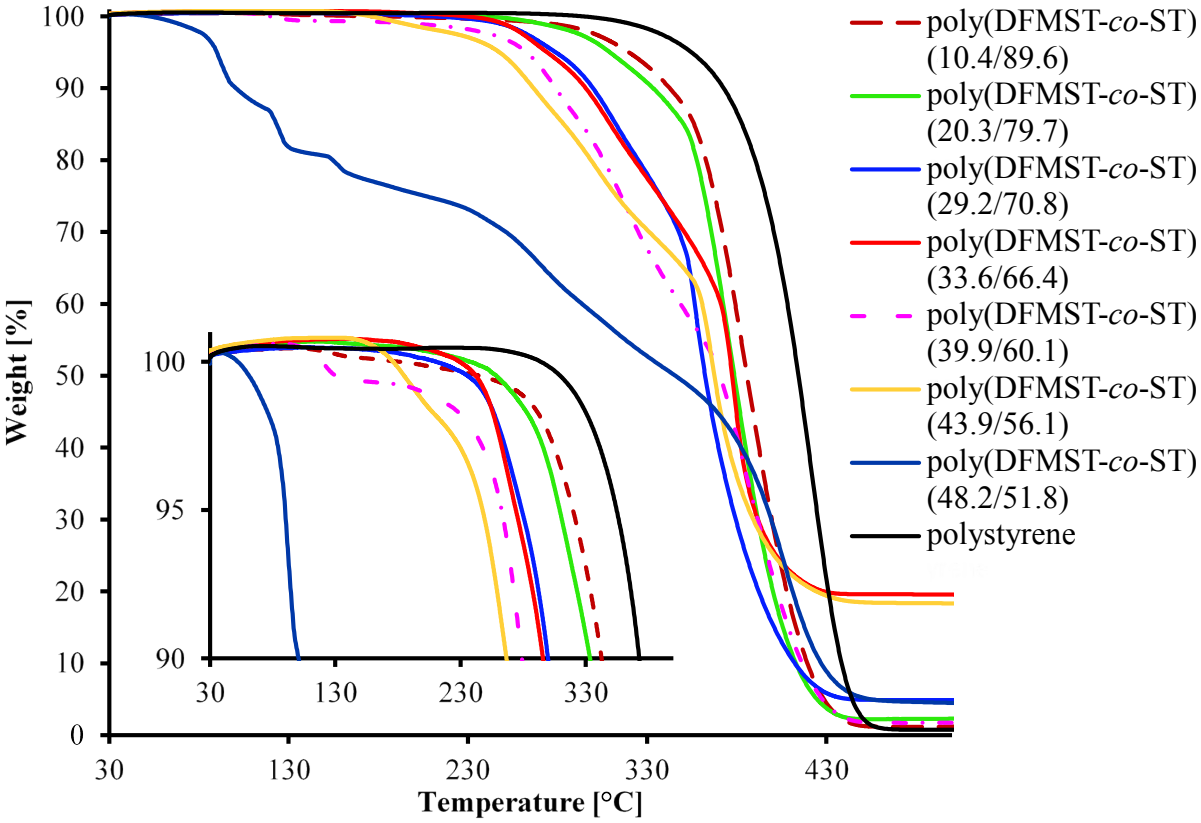

Fig. S20. TGA thermograms of series poly(DFMST-*co*-ST) copolymers with different comonomer contents in bulk radical copolymerizations.

8. Thermal Degradation Analysis

8.1. Simultaneous Thermal Analysis coupled with Fourier Transform Infrared Spectroscopy (STA/FTIR)

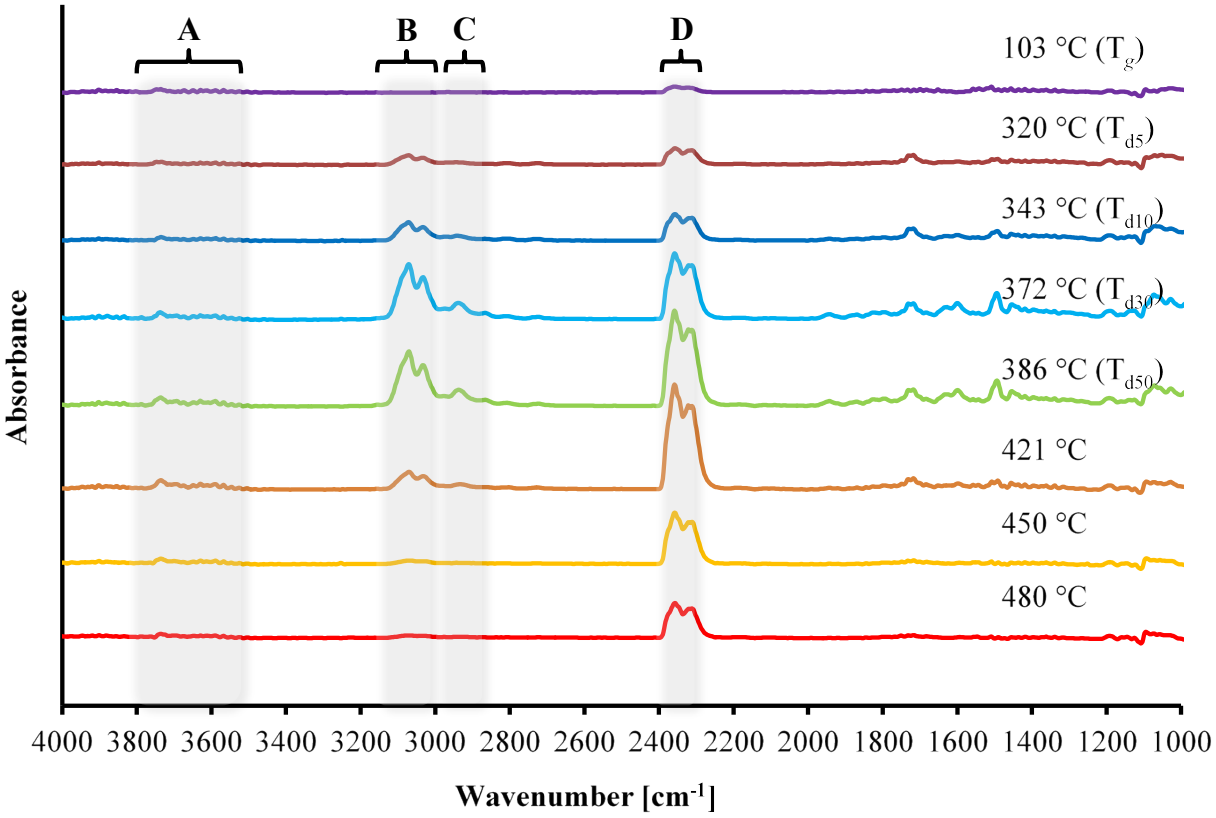

Fig. S21. FTIR spectra of gases (**A**: H_2O between 3800 and 3550 cm^{-1}; **B**: aromatic hydrocarbons between 3100 and 3010 cm^{-1}; **C**: CH_4 between 2970 and 2880 cm^{-1}; **D**: CO_2 between 2400 and 2350 cm^{-1}) evolved from the poly(DFMST-*co*-ST) copolymer (10.4/89.6) at selected temperatures.

8.2. Thermogravimetric Analysis coupled with Mass Spectrometry (TGA/MS)

a)

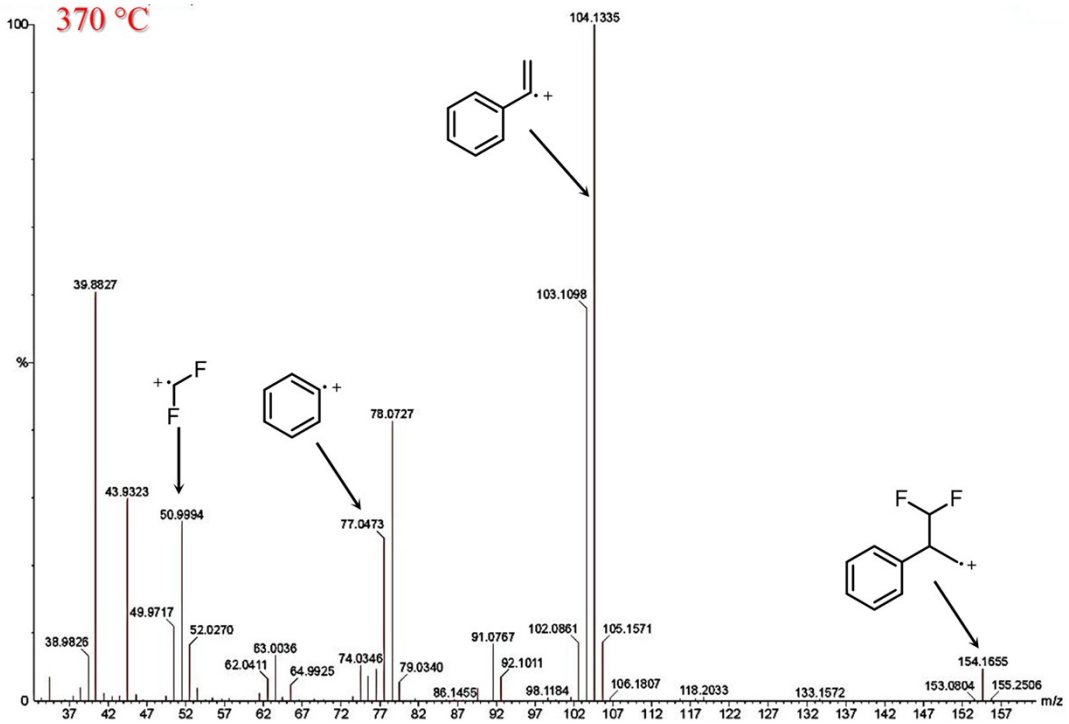

b)

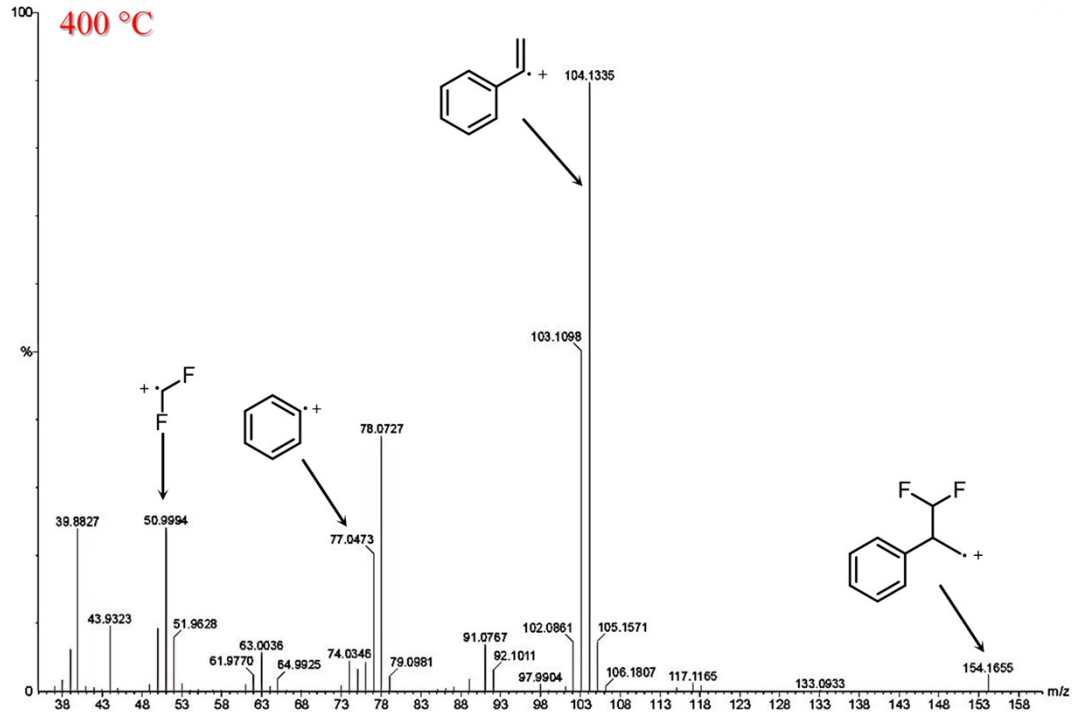

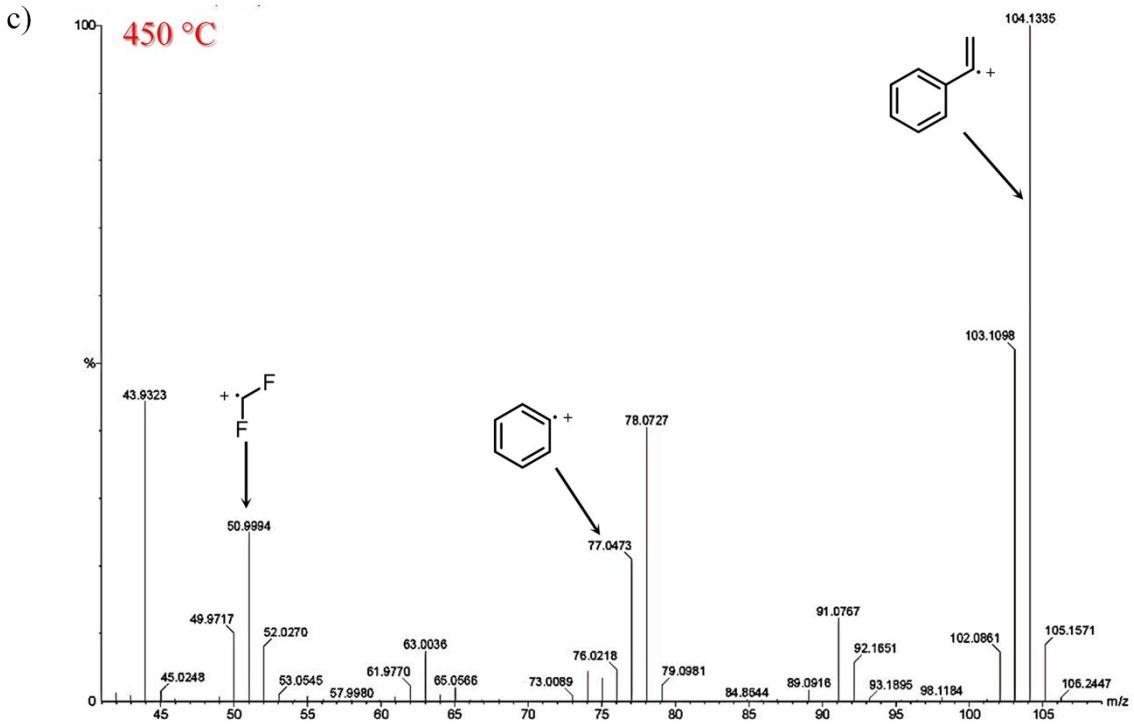

Fig. S22. Mass spectra of poly(DFMST-*co*-ST) copolymer (10.4/89.6) at the three main decomposition steps at 370 °C (a), 400 °C (b) and 450 °C (c), measured using TGA/MS analysis.

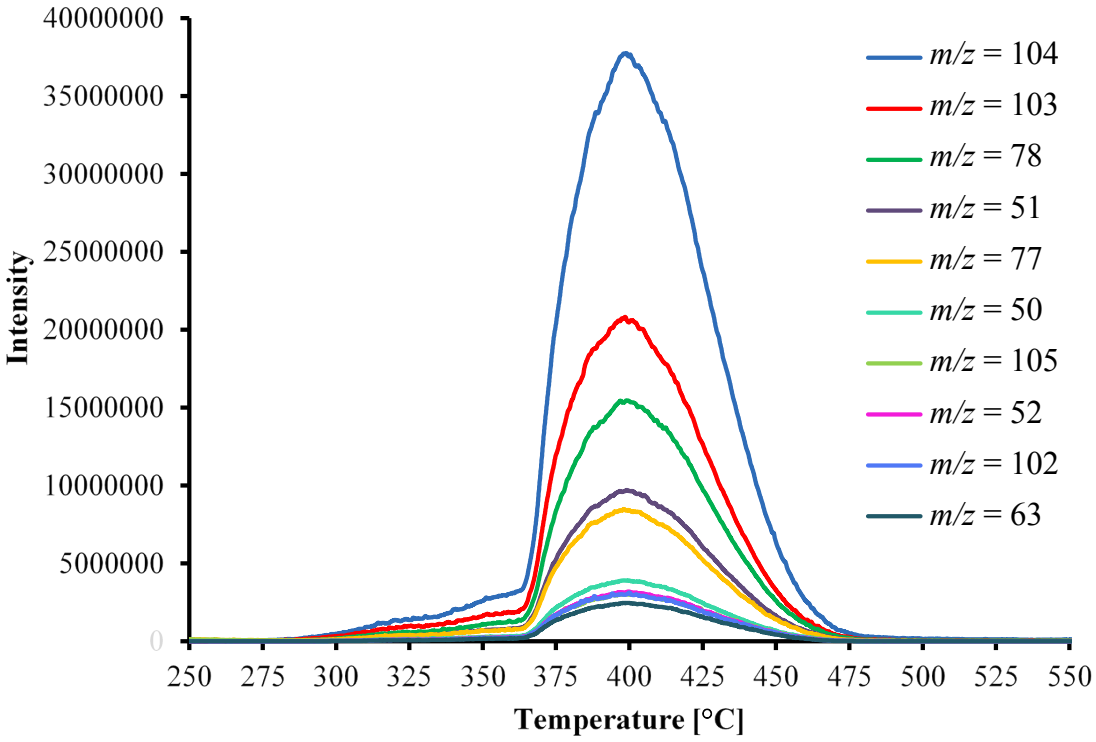

Fig. S23. Evolution of *m/z* signals of styrene from thermal decomposition of poly(DFMST-*co*-ST) copolymer (10.4/89.6).

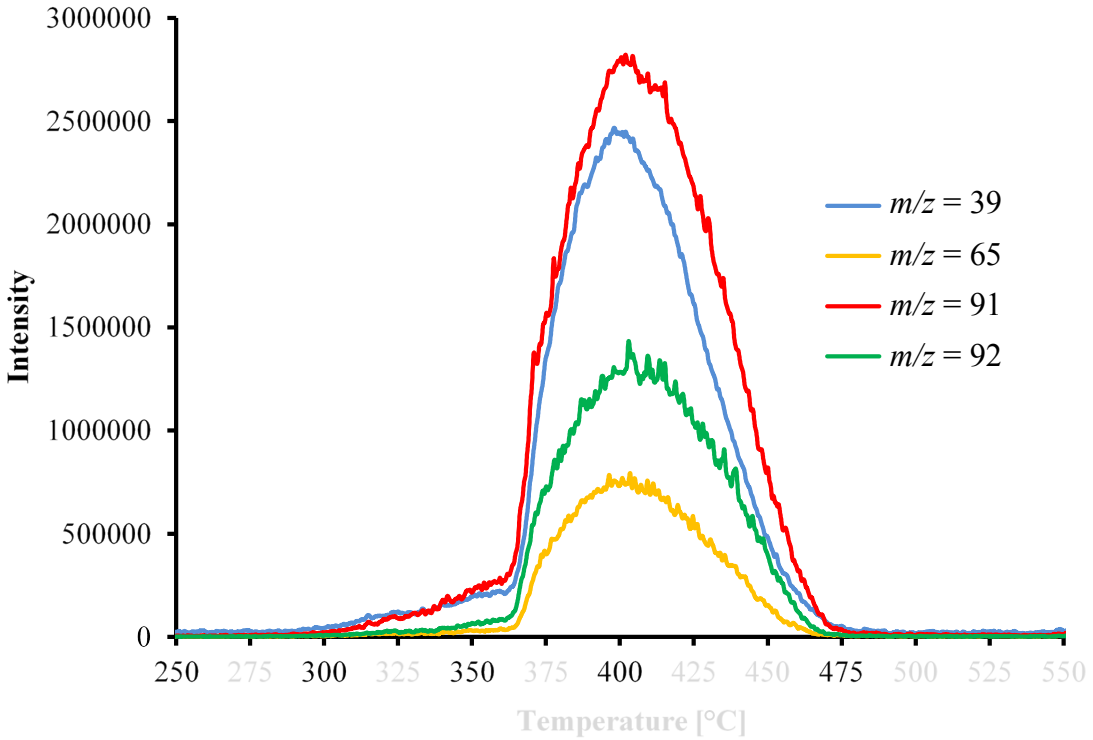

Fig. S24. Evolution of *m/z* signals of toluene from thermal decomposition of poly(DFMST-*co*-ST copolymer (10.4/89.6).

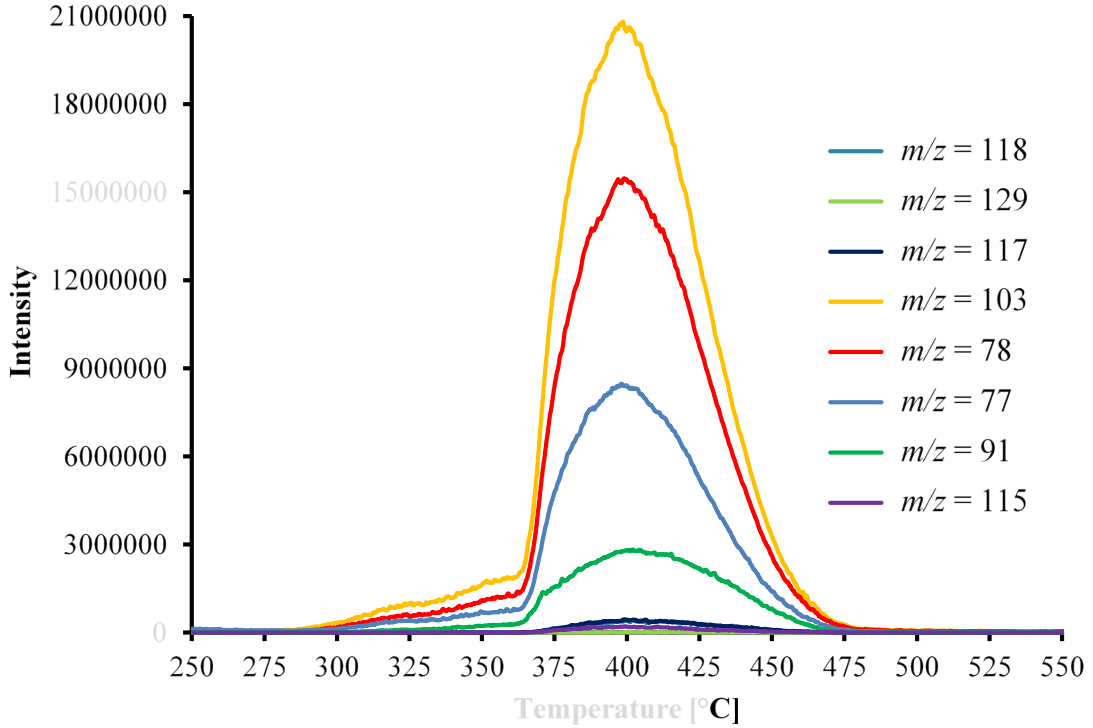

Fig. S25. Evolution of *m/z* signals of *α*-methylstyrene from thermal decomposition of poly(DFMST-*co*-ST) copolymer (10.4/89.6).

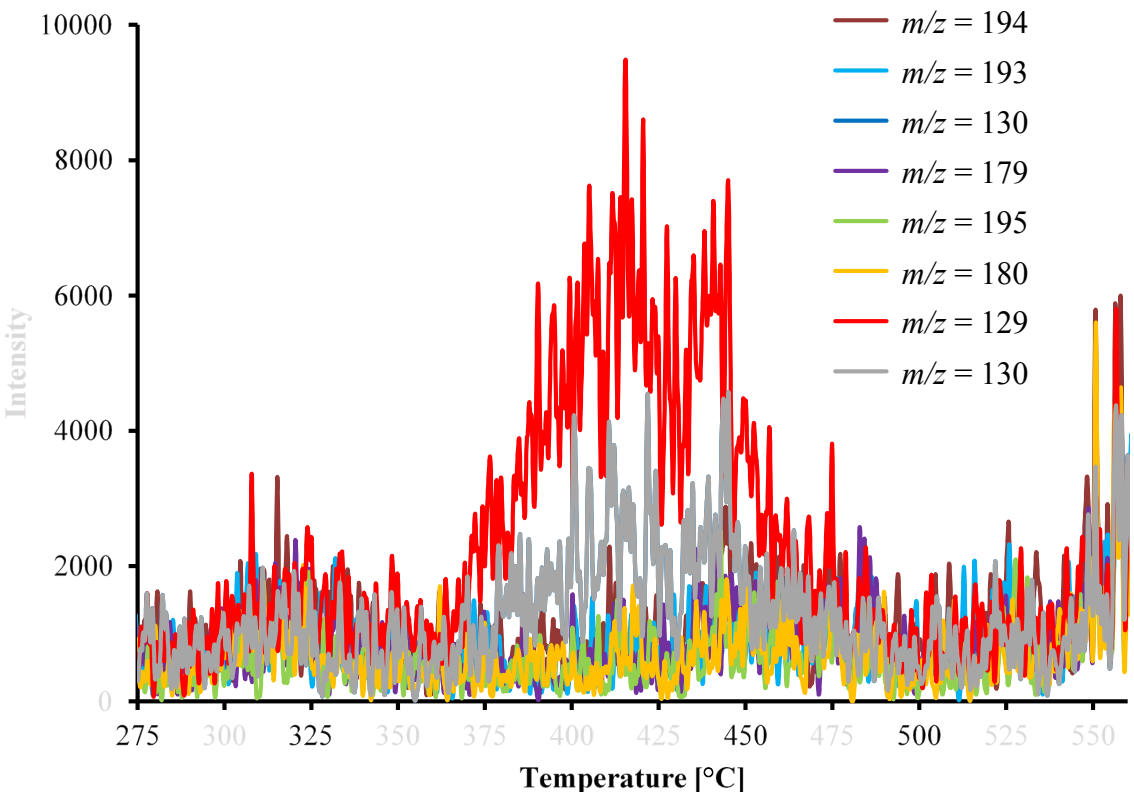

Fig. S26. Evolution of *m/z* signals of styrene dimer from thermal decomposition of poly(DFMST-*co*-ST copolymer (10.4/89.6).

9. References

(1) Walkowiak, J.; Martinez Del Campo, T.; Ameduri, B.; Gouverneur, V. Syntheses of Mono-, Di-, and Trifluorinated Styrenic Monomers. *Synthesis (Stuttg).* **2010**, *11*, 1883–1890.

(2) Prakash, G. K. S.; Hu, J.; Olah, G. A. Preparation of Tri- and Difluoromethylsilanes via an Unusual Magnesium Metal-Mediated Reductive Tri- and Difluoromethylation of Chlorosilanes Using Tri- and Difluoromethyl Sulfides, Sulfoxides, and Sulfones. *J. Org. Chem.* **2003**, *68*, 4457–4463.

(3) Walkowiak-Kulikowska, J.; Kanigowska, J.; Koroniak, H. α-(Difluoromethyl)styrene: Improved Approach to Grams Scale Synthesis. *J. Fluor. Chem.* **2015**, *179*, 175–178.